Visualization of Intraaneurysmal Flow Patterns with Transluminal Flow Images of 3D MR Angiograms in Conjunction with Aneurysmal Configurations

Toru Satoh, Keisuke Onoda, and Shoji Tsuchimoto

BACKGROUND AND PURPOSE: How the complex flow phenomena generated within unruptured cerebral aneurysms relate to the corresponding aneurysmal geometry is unknown. To estimate the interaction between flow patterns and morphologic features of unruptured cerebral aneurysms, we developed a method to visualize intraanuerysmal flow patterns with transluminal flow imaging of 3D MR angiograms in conjunction with aneurysmal configurations.

METHODS: Transluminal images of the vessel lumen were reconstructed with use of a parallel volume-rendering algorithm by selecting information on the margin of lumina from the volume data sets of 3D time-of-flight MR angiograms. Transluminal flow images were then created by superimposing flow-related intraluminal information onto transluminal images. Intraaneurysmal flow patterns were evaluated in three cases of unruptured cerebral aneurysms, based on the animated display of transluminal flow images with stepwise extracted intraluminal volume data of signal intensity, in conjunction with the corresponding aneurysmal configurations depicted on 3D MR angiograms.

RESULTS: Transluminal flow images showed 3D visualization of flow-related signal intensity distribution obtained from volume data of MR angiograms, so that qualitative information regarding intraaneurysmal flow patterns could be estimated with respect to morphologic features of cerebral aneurysms.

CONCLUSION: Transluminal flow images of 3D MR angiograms allowed feasible visualization of intraaneurysmal flow patterns that were studied. More work is required to validate the technique and clarify the significance of being able to visualize intraaneurysmal flow patterns.

Numerous flow dynamics studies of cerebral aneurysms have been conducted in experimental models and clinical trials to investigate the role of hemodynamic forces in the initiation, growth, and rupture of cerebral aneurysms (1–7). In individual clinical cases with unruptured cerebral aneurysms, however, the relationship of the complex flow phenomena generated within cerebral aneurysms to the corresponding aneurysmal geometry is not known; also unknown is the relationship between a change in flow dynamics and growth and rupture of an aneurysm with time course.

As a noninvasive screening method, current advances in CT and MR imaging provide invaluable volume data on the angioarchitecture of cerebral aneurysms, which has had a positive effect on the therapeutic management of cerebral aneurysms (8–11). Three-dimensional reconstruction of luminal data, shown by CT and MR angiograms, represents the anatomic spatial relationship and morphologically fine configuration of the parent arteries and an aneurysm. By using reconstruction software for computer visualization applied to the workstation, it is possible to select specific and limited data from the whole-volume data sets, based on the opacity chart of CT values or MR signal intensities (12, 13). By selecting the data obtained from intraluminal information, the intraaneurysmal flow patterns may be represented and analyzed in relation to the morphologic features of the aneurysmal angioarchitecture.

We have developed a transluminal imaging tech-

nique for visualization of an object transparently through the vessel lumen, by using 3D CT and MR angiograms, in which information of the outer margin of the vessel lumen is selected from the volume data set and represents the contour of the vessels and aneurysms as a series of rings (12, 13). Transluminal imaging allows a transluminal view from outside or inside the vessel lumen through the spaces between the rings and provides direct visualization of the underlying objects through the lumina. Further, to visualize the flow patterns, we developed a transluminal flow imaging technique in which the flow-related intraluminal information is simply superimposed onto transluminal angiograms. The transluminal flow images of 3D MR angiograms represent qualitative information regarding intraaneurysmal flow patterns as a relative change in spatial distribution of MR signal intensities within an aneurysm in conjunction with corresponding aneurysmal configuration.

In the present study, we evaluated our initial results of applying transluminal flow imaging of 3D MR angiograms in three cases of unruptured cerebral aneurysms. Intraaneurysmal flow patterns were visualized and evaluated by the animated display of transluminal stepwise flow images in conjunction with aneurysmal configurations.

Methods

MR Angiogram Data Acquisition

We studied three cases of unruptured cerebral aneurysm detected incidentally at MR angiography: two cases of internal carotid–posterior communicating artery aneurysm and one case of internal carotid–ophthalmic artery aneurysm. We used 1.0-T superconducting MR imaging equipment (Signa HiSpeed; GE Medical Systems, Milwaukee, WI) for MR angiography. Images were obtained with a 3D time-of-flight, spoiled gradient-recalled acquisition in the steady state sequence, without cardiac or respiratory gating. Imaging protocol was as follows: 35/3.9–4.1/2 (TR/TE/NEX), flip angle 20°, 192 × 128 matrix, 1.2-mm thickness, 0.6-mm section interval,16-cm field of view, without magnetization transfer contrast, total imaging time 8 minutes 49 seconds (two slabs), 60 sections in total (two slabs), zero-fill interpolation processing two times, overlap of eight sections. A total of 104 source axial images were obtained, and those volume data were transferred to a workstation (Zio M900; AMIN Co. Ltd., Tokyo, Japan).

Reconstruction of Transluminal 3D MR Images

The data were reconstructed every 0.3 mm on a workstation, then processed into a 3D volume-rendering data set in 9 seconds. The 3D MR angiograms were created from the data set in 11 seconds by the conventional parallel volume-rendering algorithm, by using an increasing curve starting with a threshold of 145 (0% opacity level) and up to 155 (100% opacity level)(Fig 1, top). Based on a signal intensity corresponding to the luminal margin on the source images, transparency of the luminal wall was selected from the opacity chart of MR signal intensities by using a spiked peak curve with a threshold range of 145–155 (peak value at 150 with 100% opacity level, window width 10) (Fig 1, middle). The resultant transluminal 3D MR angiogram (data reconstructed in 11 seconds) represented the contour of the vessel and aneurysmal configurations as a series of rings (color-rendered in red-purple in Fig 1).

Reconstruction of Transluminal Flow Images of 3D MR Angiograms

To create the transluminal flow image, intraluminal volume data, shown by regions of signal intensity distribution, were simply superimposed onto the transluminal 3D MR angiogram and reconstructed in 11 seconds. The data were selected stepwise by using another square curve from the opacity chart of MR signal intensities used for the transluminal image. The intraluminal data were extracted in 30 increments with threshold ranges of 350–500, 320–500, 290–500, 260–500, 230–500, and 200–500 (100% opacity level, respectively) (color-rendered in pink in Fig 1, bottom). Serial change in stepwise extracted intaluminal contents within a transluminal image was evaluated continuously by the animated display and used to estimate intraaneurysmal flow patterns in conjunction with aneurysmal configurations.

Results

The transluminal 3D MR angiograms represented the configuration of the parent arteries and an aneurysm as a series of rings, also showing the neck, dome, and bleb. By using the transluminal flow images of 3D MR angiograms, intraluminal contents relating to blood flow information were superimposed onto transluminal images, and 3D distribution of intraluminal MR signal intensities was visualized transluminally through the vessel lumina. The flow pattern within an aneurysm was evaluated as a change in signal intensity distribution by animated display of transluminal stepwise flow images.

Case 1

A 75-year-old woman had an unruptured left internal carotid–posterior communicating artery aneurysm. The volume-rendered images of CT and MR angiograms showed that the aneurysm was 12.7 × 8.4 mm (Fig 2A and B). The magnified images of CT and MR angiograms depicted the aneurysm to have a bleb at the lateral tip of the dome (Fig 2C and D). The maximum intensity projection image of the CT angiogram showed homogeneous contents within the aneurysmal sac (Fig 2E). However, the maximum intensity projection image of the MR angiogram showed a high-signal-intensity linear area entering at the distal neck orifice and running along the superoposterior margin of the dome, with an area of relatively low signal intensity in most of the remaining dome, including the bleb (Fig 2F). The transluminal flow images with stepwise intraluminal contents demonstrated the flow pattern within the aneurysm (Fig 2G–L). The blood flow pattern was evaluated as follows: blood flow entered into the aneurysm from the distal aspect of the neck orifice and swirled along the superoposterior wall, with a relatively slow-flow vortex at the central zone and proximal neck within the aneurysm and very slow flow at the protrusion of the inferolateral dome and in the inferoposterior bleb.

Case 2

A 66-year-old man had an unruptured left internal carotid–posterior communicating artery aneurysm. The magnified volume-rendered CT and MR angio-
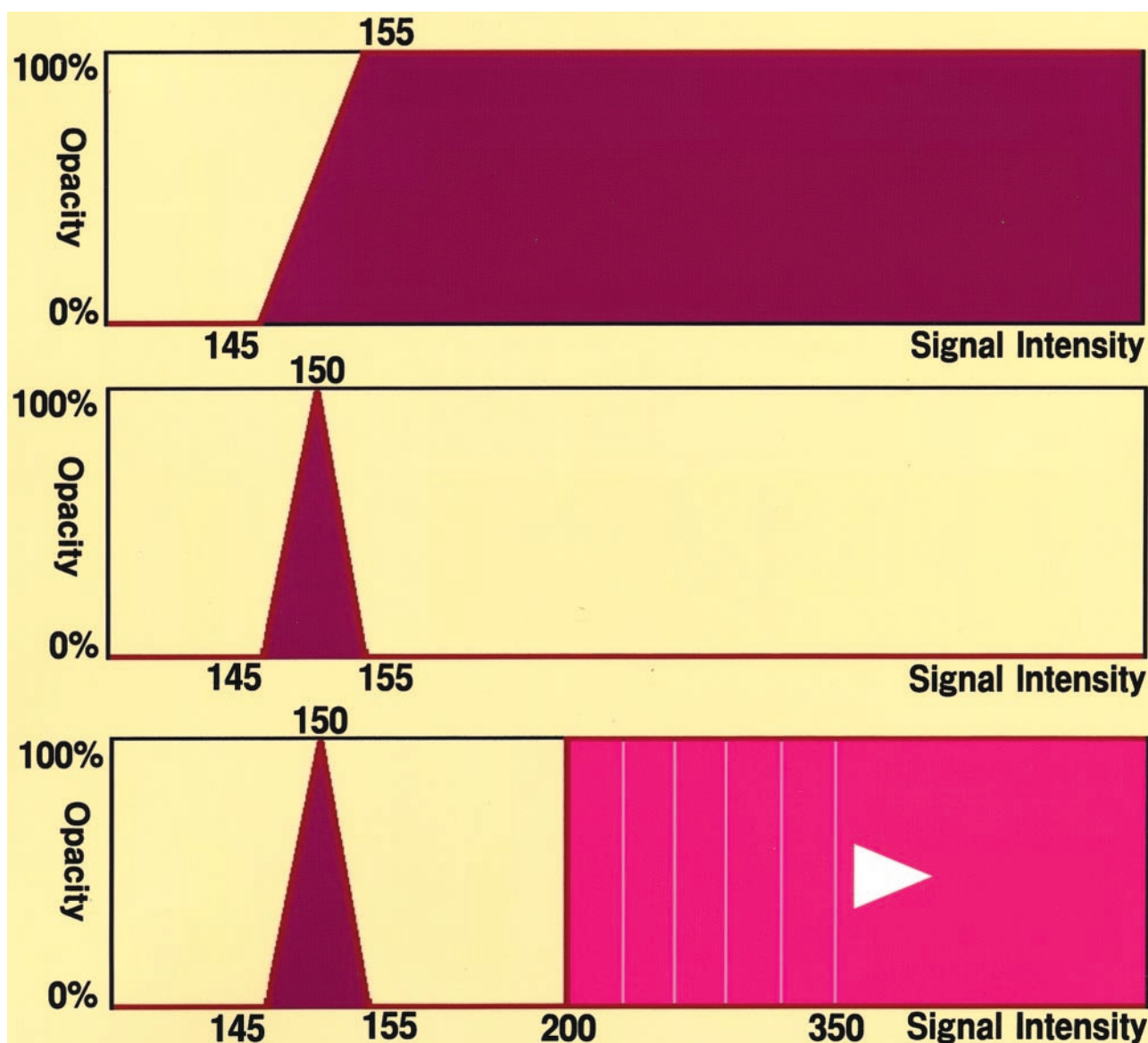
FIG 1.   Schematic illustration of selective opacity curves used in the opacity chart of MR signal intensities: increasing curve for the conventional parallel volume-rendered imaging (top), spiked peak curve for transluminal imaging (middle), and spiked peak curve with a stepwise square curve for transluminal flow imaging (bottom). Serial observation of transluminal flow images represents the intraaneurysmal flow patterns by superimposing stepwise extracted intraluminal volume data, with signal intensities ranging 350–500, 320–500, 290–500, 260–500, 230–500, and 200–500, respectively, onto the corresponding transluminal images with aneurysmal configurations.

grams showed the aneurysm (11.3 × 8.5 mm) to have a bleb at the medial aspect of the dome (Fig 3A and B). The maximum intensity projection image of the CT angiogram showed relatively homogeneous contents within the aneurysmal sac (Fig 3C). However, the maximum intensity projection image of the MR angiogram showed a high-signal-intensity linear area entering at the distal neck orifice and running along the superoposterior margin of the dome, with an area of relatively low signal intensity in most of the remaining dome (Fig 3D). The digital subtraction angiograms obtained in the early and late arterial phases showed that the aneurysm had inhomogeneous intraaneurysmal contents (Fig 3E and F). Contrast medium was distributed mainly at the superoposterior

area within the dome, consistent with blood flow within the aneurysm. The transluminal flow images of the 3D MR angiogram with stepwise intraluminal contents demonstrated the flow pattern within the aneurysm (Fig 3G–L). The blood flow entered into the aneurysm from the distal side of the orifice and flowed along the superoposterior wall, with relatively slow flow at the center and most of the remaining part of the dome. Very slow flow was shown at the inferomedial region, including the bleb.

Case 3

63-year-old woman had an unruptured left internal carotid–ophthalmic artery aneurysm. The magnified
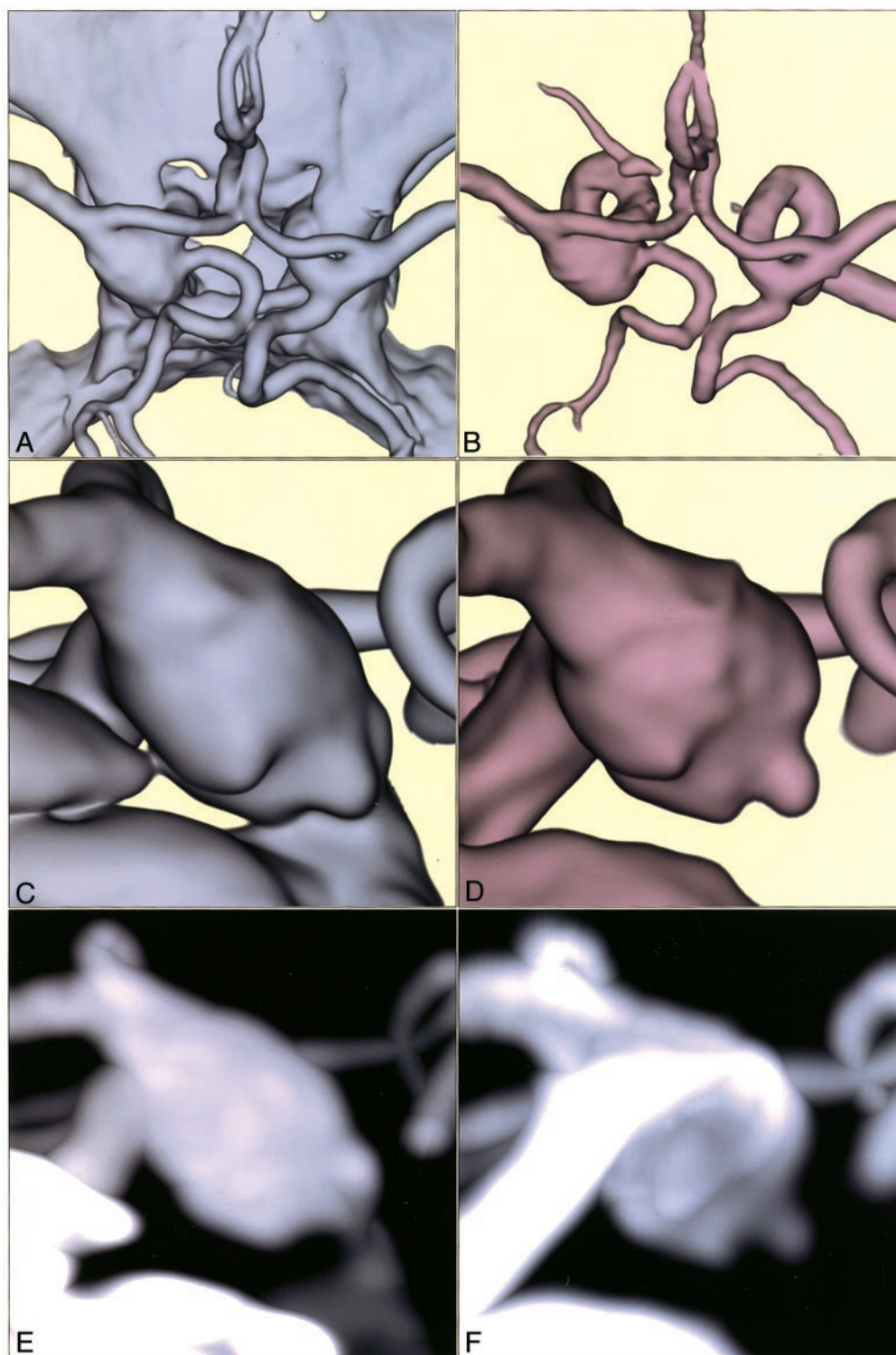
FIG 2. Case 1. 75-year-old woman with an unruptured left internal carotid–posterior communicating artery aneurysm.
 A and B, Three-dimensional volume-rendered CT and MR angiograms, respectively, superoinferior projection.
 C and D, magnified images of CT and MR angiograms, respectively, left lateral projection.
 E and F, Maximum intensity projection images of CT and MR angiograms, respectively. *Figure 2 continues.*
 Figure 2 continued. G–L, Transluminal flow images of 3D MR angiogram with stepwise intraluminal contents, with signal intensities ranging 350–500, 320–500, 290–500, 260–500, and 200–500, respectively, demonstrate blood flow as the three-dimensional distribution of signal intensities.

volume-rendered MR angiogram and coordinated maximum intensity projection image showed that the aneurysm (9.2 × 10.4 mm) extended medially (Fig 4A and B). The transluminal flow images of the 3D MR angiogram with stepwise intraluminal contents demonstrated the flow pattern within the aneurysm (Fig
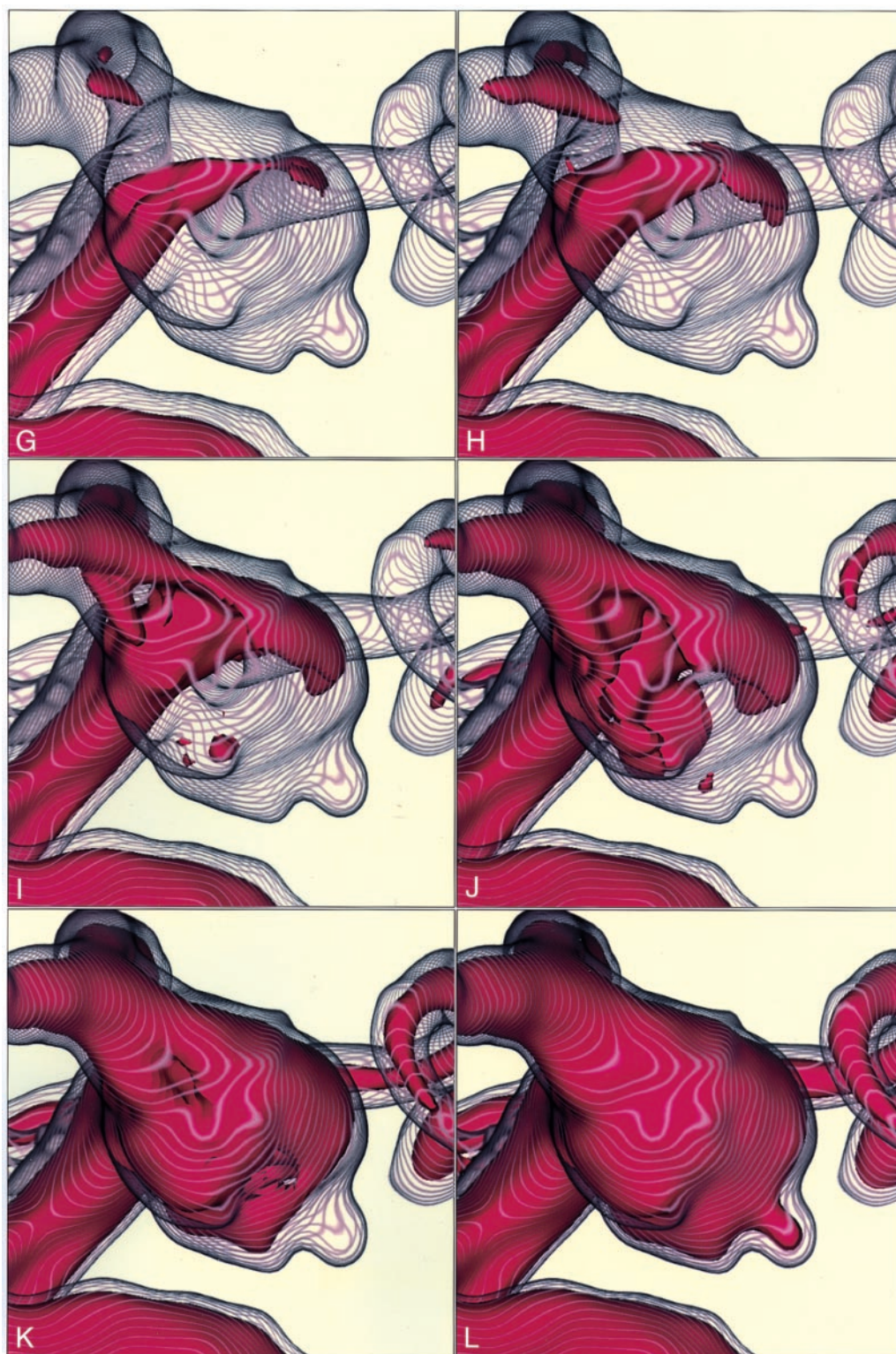
Figure 2. *Continued*.

4C–F). The blood flow entered into the aneurysm from the distal side of the orifice and flowed along the posterosuperomedial wall, with relatively slow flow at the center and remaining anteroinferomedial part of the dome to the proximal side of the orifice.

Discussion

With use of MR and helical CT angiography for screening and further examination of cerebrovascular diseases, a number of unruptured cerebral aneurysms can be detected incidentally. Because the natural his-
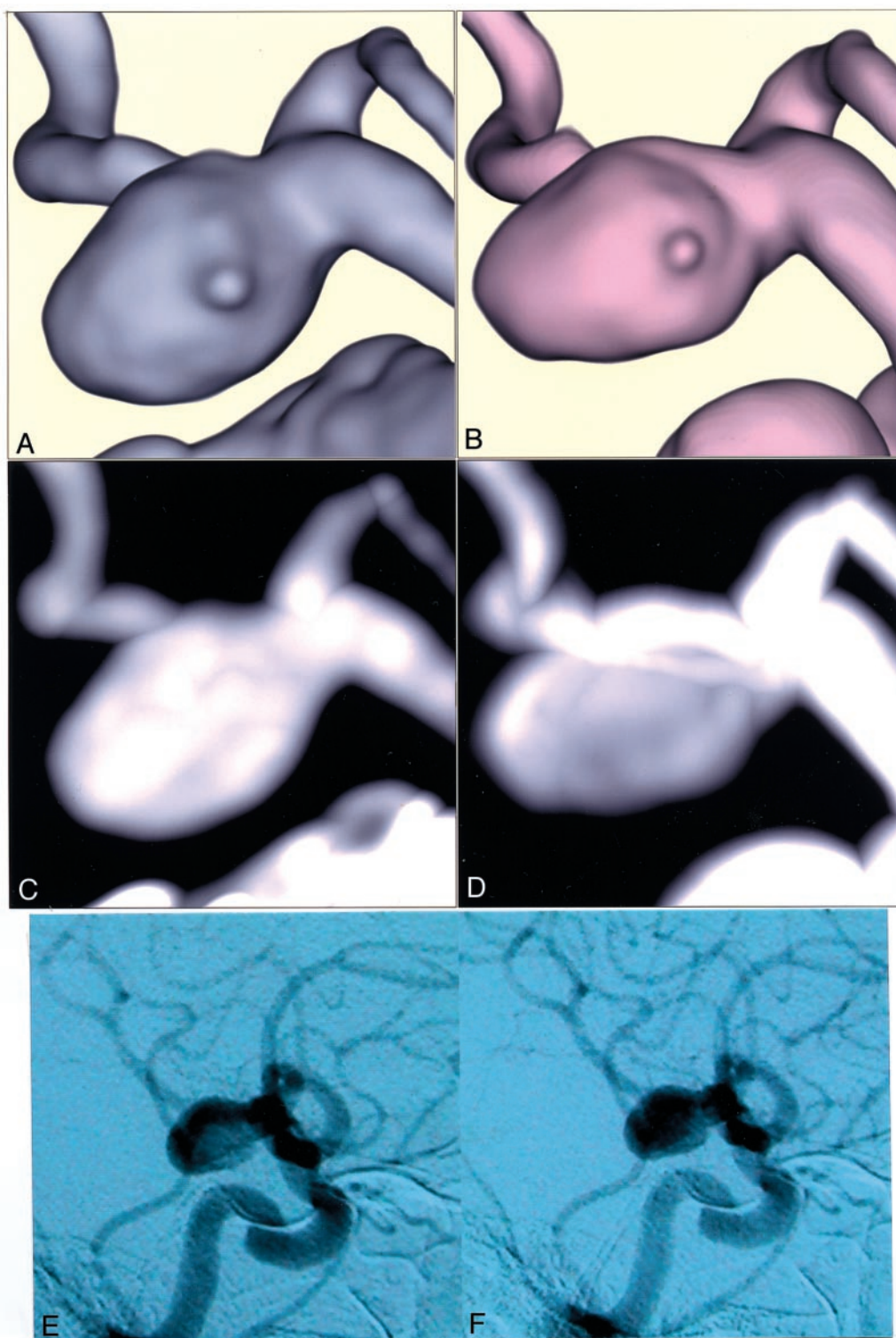
FIG 3.   Case 2. 66-year-old man with an unruptured left internal carotid–posterior communicating artery aneurysm.
   A and B, Magnified volume-rendered CT and MR angiograms, respectively, right lateral projection.
   C and D, Maximum intensity projection images of CT and MR angiograms, respectively. E and F, Digital subtraction angiograms, lateral projection, obtained in the early and late arterial phases, respectively. Figure 3 continues.
   Figure 3 continued. G–L, Transluminal flow images of 3D MR angiogram with stepwise intraluminal contents, with signal intensities ranging 350–500, 320–500, 290–500, 260–500, 230–350, and 200–500, respectively.

tory of unruptured cerebral aneurysms is unknown, it remains controversial whether such aneurysms should be prophylactically treated by surgical and interven-tional procedures or observed conservatively (14–21). The size, shape, and location of unruptured cerebral aneurysms are reported to be the most reliable ana-
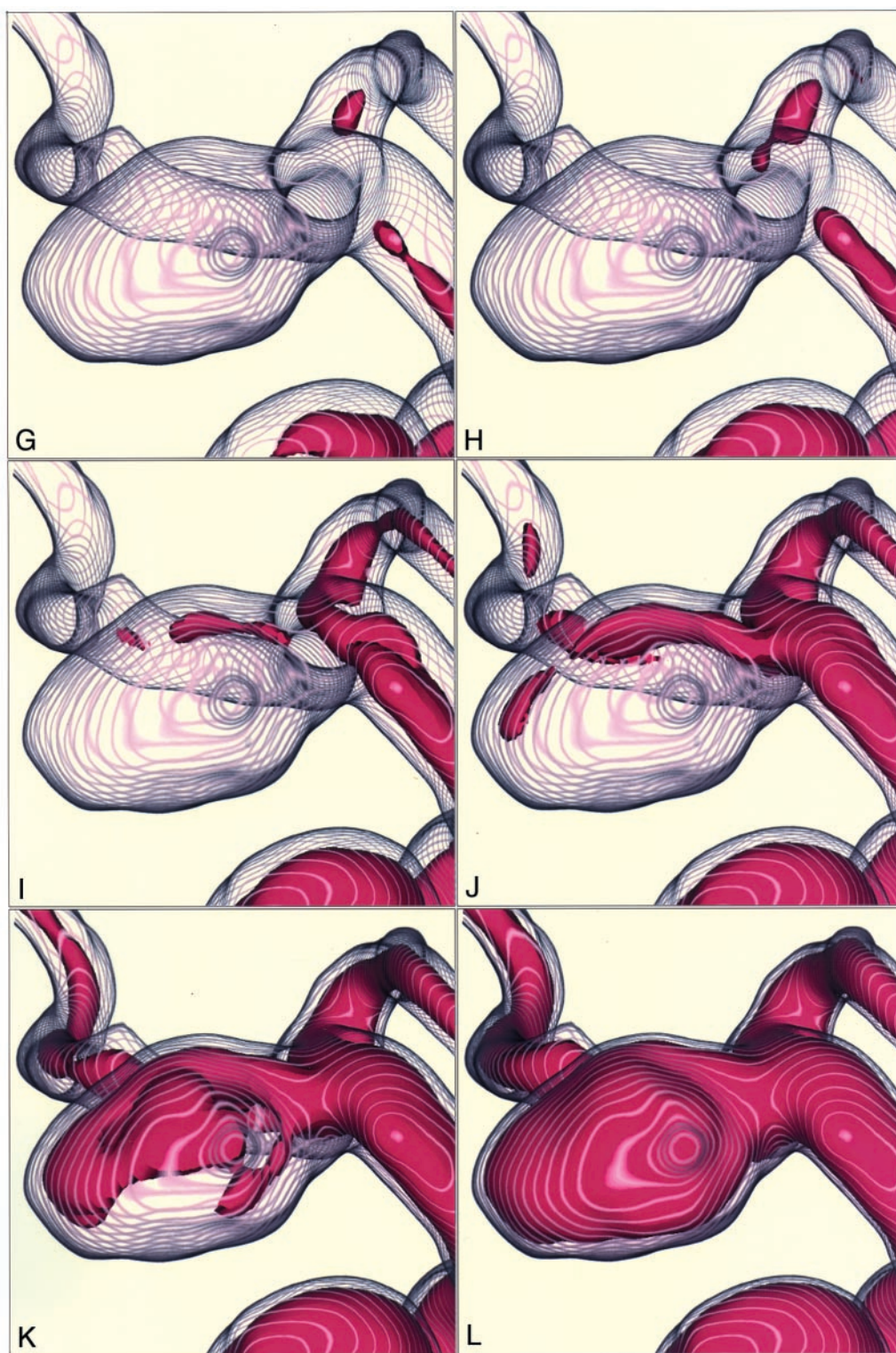
FIGURE 3. CONTINUED.

tomic risk factors for rupture (15–19, 21). In recent studies, it has been suggested that physiologic factors, such as intraaneurysmal blood velocity, blood pressure, asymmetric flow state, and fluid-induced wall shear stress may be responsible for the development and growth of aneurysms (1–7, 22–24).

Intraluminal Information on CT and MR Angiograms

CT angiograms provide luminal volume data by filling the vessel lumen with contrast medium and depict the luminal morphologic configuration of the
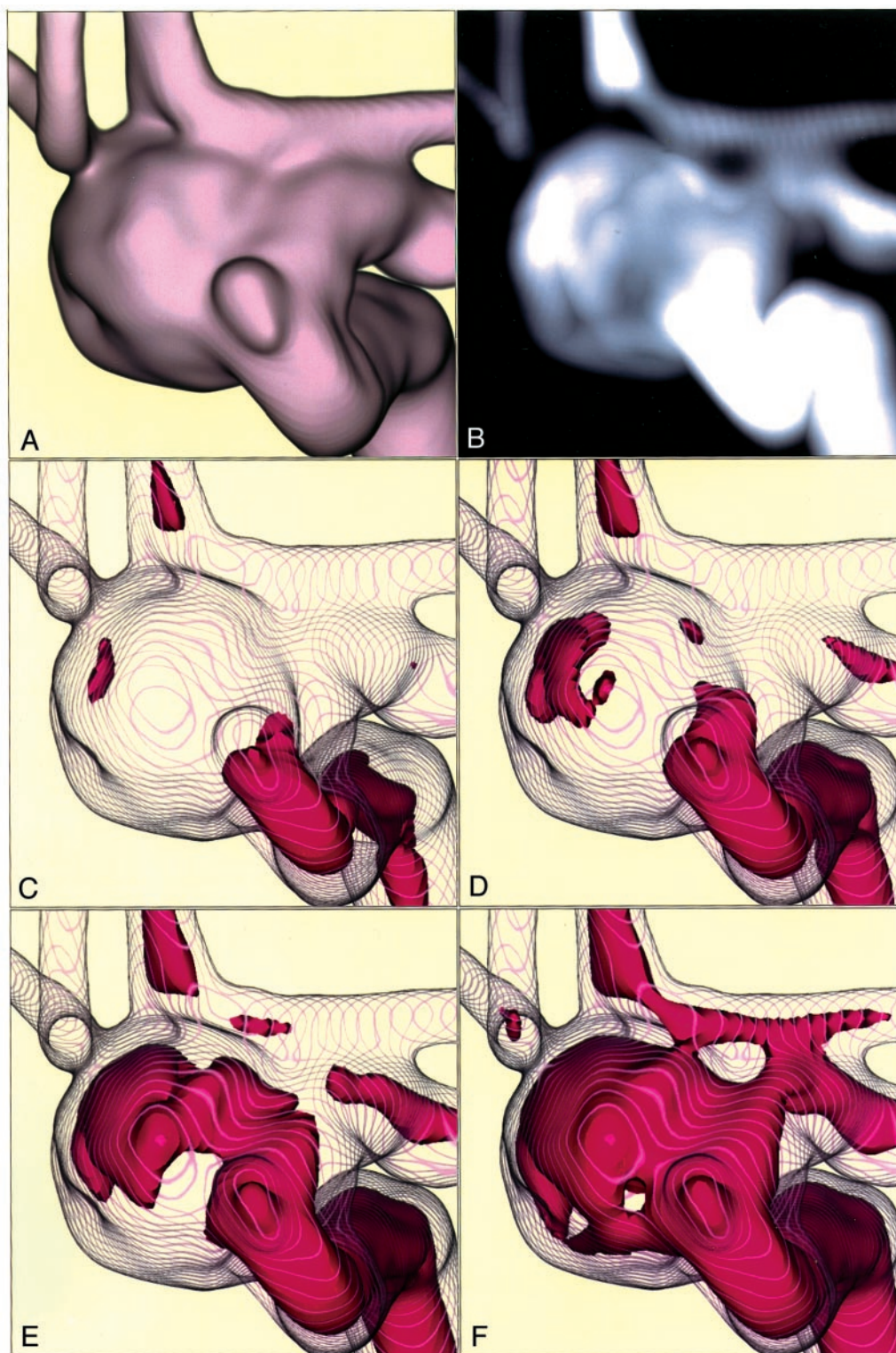
FIG 4. Case 3. 63-year-old woman with an unruptured left internal carotid–ophthalmic artery aneurysm.
A, Magnified volume-rendered MR angiogram and *B,* coordinated maximum intensity projection image, anteroposterior projection.
C–F, Transluminal flow images of 3D MR angiogram with stepwise intraluminal contents, with signal intensities ranging 350–500, 320–500, 290–350, and 260–500, respectively.

parent arteries and an aneurysm; this representation is similar to that obtained with digital subtraction angiography (5, 9, 12). Intraluminal information indicated by CT values consists of the volume of contrast

medium delivered from blood flow during the scanning period.

In contrast, volume data of MR angiography, obtained by 3D time-of-flight data acquisition, represent

flow voids related mainly to peak inflow velocity within the vessel lumen during data acquisition (8, 10, 11, 13, 25, 26). Intraluminal functional blood flow information on MR angiograms, however, is complicated and affected by several factors. Loss of signal intensity occurs mainly from spin saturation effects due to slow flow, and/or phase dispersion due to disturbed and complex flow (10, 25, 26). The fundamental patterns of flow within the aneurysm are composed of inflow, circulating flow, and outflow (2, 3, 6, 7, 22). Depending on the aneurysmal geometry, including the size of the neck and the flow ratio in distal branches, complex intraaneurysmal flow phenomena are generated by circulating flow, recirculating flow, and stagnation or stasis of flow (3, 6). Slow or disturbed flow conditions within the aneurysm may cause a decrease in MR signal intensity. Complex intraaneurysmal flow results in inaccurate contour of an aneurysm with inhomogeneous intraaneurysmal contents depicted on the maximum intensity projection images or the source images of MR angiograms, as compared with morphologic features shown on CT angiograms. With respect to flow-related information, however, heterogeneous intraluminal signal intensity distributions, caused by signal intensity loss on MR angiograms, may provide specific and characteristic features relating to the intraaneurysmal blood flow patterns.

Evaluation of Intraaneurysmal Flow Patterns on Transluminal Flow Images of 3D MR Angiograms

The transluminal images of 3D MR angiograms represent the marginal information selected from luminal volume data, which consist of the vessels and aneurysms shown as a series of rings (12, 13). In the present study, we extracted the intraluminal information by selecting the volume data according to the signal intensities obtained on MR angiograms. Selected information related to intraluminal blood flow was simply superimposed onto transluminal images.

With this transluminal flow image, it was possible to visualize flow-related information within the lumen through the spaces between the rings of the lumina consisting of aneurysmal configurations.

Flow patterns within an aneurysm were analyzed based on the animated display of transluminal flow images with stepwise extracted intraluminal volume data. Continuous observation of the flow-related information depicts the 3D signal intensity distributions as a pattern of blood flow. From another approach, stereoscopic or multiprojection views of the transluminal flow images could enhance the realistic spatial distribution of the intraaneurysmal flow patterns.

Transluminal flow images represent flow as calculated from peak systolic velocities, but because of the complex pulse wave in the intracranial circulation, this representation likely is a considerable oversimplification of actual flow. Because the flow within aneurysms likely varies in complexity according to the heart rate, intraaneurysmal flow patterns illustrated

by transluminal flow images may change with variations in heart rate.

Limitations of Flow Pattern Evaluation with Transluminal Flow Images of MR Angiograms

There are several limitations to the evaluation and analysis of intraaneurysmal blood flow patterns with 3D MR angiographic transluminal flow images. First, because MR signal intensity of volume data, obtained by 3D time-of-flight acquisition, varies among individuals and conditions of examination, the absolute value for blood flow is difficult to define. By using contrast material–enhanced 2D cine phase MR angiography, quantitative change in blood flow velocity is measured during systolic and diastolic cardiac phases (27), but the range of interest is very small and restricted within the basilar artery. In addition, cardiac gating may be necessary for investigating pulsatile effects on blood flow and aneurysm (23). Quantitative evaluation of actual flow is difficult; however, qualitative information or relative change regarding intraaneurysmal flow patterns may be possible to evaluate with transluminal flow images of 3D MR angiograms on a case-specific basis, incorporating the anatomic geometry of an aneurysm.

The second limitation is related to reconstruction of image data by using the volume-rendering technique (8–10, 12, 13). The diameter of the lumen, consisting of a series of rings, is variable depending on the MR signal intensities selected for the vessel wall, so the threshold range of the opacity curve selected for the aneurysmal wall must be optimized based on the source axial images. In a case of an aneurysm containing thrombus or heavy calcification in a portion of its wall, analysis of flow pattern may be affected by poor information on source images.

The third limitation depends on the characteristics of volume information on MR angiograms. Volume data obtained by MR angiography provide flow-related functional information, and images of vessels and aneurysms on MR angiograms are similar to but different from the morphologic features shown on CT or digital subtraction angiograms. The outer margin of the lumen on transluminal images of MR angiograms did not represent the true contours of the vessels and aneurysmal walls, which resulted in a certain discrepancy in the shape and size of an aneurysm as compared with those on CT or digital subtraction angiograms. These findings may recommend that the depiction of flow-related intraluminal information of MR angiograms be superimposed onto the projection-matched corresponding transluminal CT or digital subtraction angiograms.

Conclusion

Transluminal flow images of 3D MR angiograms can provide feasible visualization of intraluminal flow patterns of unruptured cerebral aneurysms. Qualitative information regarding intraaneurysmal flow patterns could be estimated with respect to the morpho-

logic features of the cerebral aneurysms that were studied. Pretreatment qualitative evaluation of intraaneurysmal blood flow patterns may provide another clinical factor to consider in the natural history of an unruptured cerebral aneurysm. More work is required to validate the technique and clarify the significance of being able to visualize intraaneurysmal flow patterns.

References

1. Nakatani H, Hashimoto N, Kang Y, et al. **Cerebral blood flow patterns at major vessel bifurcations and aneurysms in rats.** *J Neurosurg* 1991;74:258–262
2. Gonzalez CF, Cho YI, Ortega V, et al. **Intracranial aneurysms: flow analysis of their origin and progression.** *AJNR Am J Neuroradiol* 1992;13:181–188
3. Gobin YP, Counord JL, Flaud P, et al. **In vitro study of haemodynamics in a giant saccular aneurysm model: influence of flow dynamics in the parent vessel and effects of coil embolization.** *Neuroradiology* 1994;36:530–536
4. Burleson AC, Strother CM, Turitto VT. **Computer modeling of intracranial saccular and lateral aneurysms for the study of their hemodynamics.** *Neurosurgery* 1995;37:774–784
5. Tenjin H, Asakura F, Nakahara Y, et al. **Evaluation of intraaneurysmal blood velocity by time-density curve analysis and digital subtraction angiography.** *AJNR Am J Neuroradiol* 1998;19:1303–1307
6. Ujiie H, Tachibana H, Hiramatsu O, et al. **Effects of size and shape (aspect ratio) on the hemodynamics of saccular aneurysms: a possible index for surgical treatment of intracranial aneurysms.** *Neurosurgery* 1999;45:119–130
7. Tateshima S, Murayama Y, Villablanca JP, et al. **Intraaneurysmal flow dynamics study featuring an acrylic aneurysm model manufactured using a computerized tomography angiogram as a mold.** *J Neurosurg* 2001;95:1020–1027
8. Maeder PP, Meuli RA, de Tribolet N. **Three-dimensional volume rendering for magnetic resonance angiography in the screening and preoperative workup of intracranial aneurysms.** *J Neurosurg* 1996;85:1050–1055
9. Villablanca JP, Martin N, Jahan R, et al. **Volume-rendered helical computerized tomography angiography in the detection and characterization of intracranial aneurysms.** *J Neurosurg* 2000;93:254–264
10. Adams WM, Laitt RD, Jackson A. **The role of MR angiography in the pretreatment assessment of intracranial aneurysms: a comparative study.** *AJNR Am J Neuroradiol* 2000;21:1618–1628
11. Watanabe Z, Kikuchi Y, Izaki K, et al. **The usefulness of 3D MR angiography in surgery for ruptured cerebral aneurysms.** *Surg Neurol* 2001;55:359–364
12. Satoh T. **Transluminal imaging with perspective volume rendering of computed tomographic angiography for the delineation of cerebral aneurysms.** *Neurol Med Chir (Tokyo)* 2001;41:425–430
13. Satoh T. **Delineation of cerebral aneurysms with transluminal imaging of three-dimensional MR angiography.** *No Shinkei Geka (Tokyo)* 2001;29:951–959 [in Japanese with English abstract]
14. Winn HR, Almaani WS, Berga SL, et al. **The long-term outcome in patients with multiple aneurysms: incidence of late hemorrhage and implications for treatment of incidental aneurysms.** *J Neurosurg* 1983;59:642–651
15. Wiebers DO, Whisnant JP, Sundt TM Jr, et al. **The significance of unruptured intracranial saccular aneurysms.** *J Neurosurg* 1987;66:23–29
16. Asari S, Ohmoto T. **Natural history and risk factors of unruptured cerebral aneurysms.** *Clin Neurol Neurosurg* 1993;95:205–214
17. Rinkel GJE, Djibuti M, Algra A, et al. **Prevalence and risks of rupture of intracranial aneurysms: a systemic review.** *Stroke* 1998;29:251–256
18. International Study of Unruptured Intracranial Aneurysms Investigators. **Unruptured intracranial aneurysms: risk of rupture and risks of surgical intervention.** *N Engl J Med* 1998;340:1439–1442
19. Juvela S, Porras M, Poussa K. **Natural history of unruptured intracranial aneurysms: probability of and risk factor for aneurysm rupture.** *J Neurosurg* 2000;93:379–387
20. Tsutsumi K, Ueki K, Morita A, et al. **Risk of rupture from incidental cerebral aneurysms.** *J Neurosurg* 2000;93:550–553
21. Weir B, Disney L, Karrison T. **Size of rupture and unruptured aneurysms in relation to their sites and the age of patients.** *J Neurosurg* 2002;96:64–70
22. Kerber CW, Imbesi SG, Knox K. **Flow dynamics in a lethal anterior communicating artery aneurysm.** *AJNR Am J Neuroradiol* 1999;20:2000–2003
23. Meyer FB, Huston J III, Riederer SS. **Pulsatile increase in aneurysm size determined by cine phase-contrast MR angiography.** *J Neurosurg* 1993;78:879–883
24. Benndorf G, Wellnhofer E, Lanksch W, et al. **Intraaneurysmal flow: evaluation with Doppler guidewires.** *AJNR Am J Neuroradiol* 1996;17:1333–1337
25. Sevick RJ, Tsuruda JS, Schmalbrock P. **Three-dimensional time-of-flight MR angiography in the evaluation of cerebral aneurysms.** *J Comput Assist Tomogr* 1990;14:874–881
26. Isoda H, Ramsey RG, Takehara Y, et al. **MR angiography of aneurysm models of various shapes and neck sizes.** *AJNR Am J Neuroradiol* 1997;18:1463–1472
27. Kato T, Indo T, Yoshida E, et al. **Contrast-enhanced 2D cine phase MR angiography for measurement of basilar artery blood blow in posterior circulation ischemia.** *AJNR Am J Neuroradiol* 2002;23:1346–1351